2013 IEEE 10th International Symposium on Biomedical Imaging:
From Nano to Macro
San Francisco, CA, USA, April 7-11, 2013

COMPRESSED SENSING HARDI VIA ROTATION-INVARIANT CONCISE DICTIONARIES, FLEXIBLE K-SPACE UNDERSAMPLING, AND MULTISCALE SPATIAL REGULARITY

Suyash P. Awate

Scientific Computing and Imaging Institute,
University of Utah.

Edward V. R. DiBella

Utah Center for Advanced Imaging Research,
University of Utah.

ABSTRACT

Current methods to reduce acquisition time for high angular resolution diffusion imaging (HARDI) (i) employ large dictionaries where atoms explicitly model finitely-many tract orientations, limiting estimation accuracy of the true tract orientation, (ii) subsample gradient directions only, ignoring k-space undersampling for diffusion-weighted images, (iii) restrict to sparse models that use either frames or dictionaries, and (iv) enforce spatial regularity by penalizing total variation. This paper proposes *rotation-invariant dictionaries*, enabling a concise dictionary (few atoms representing key diffusion-signal types) by explicitly optimizing the rotation for each atom during sparse fitting. The proposed framework generalizes undersampling strategies to both k-space and gradient directions, thereby enabling a *balanced undersampling of k-space* over all directions. This paper *combines frames and dictionaries* for sparse modeling HARDI images. The frame model reduces the need for large intricate dictionaries and enforces *spatial regularity over multiple scales*. Results on simulated and clinical undersampled HARDI show improved reconstructions via the proposed framework.

Index Terms— HARDI, reconstruction, compressed sensing, k-space undersampling, dictionaries, frames.

1. INTRODUCTION AND RELATED WORK

High angular resolution diffusion imaging (HARDI) [1] enables accurate estimation of the brain's neural structure through high-resolution investigation of the anisotropic diffusion within white matter. HARDI acquires a large number of diffusion-weighted (DW) magnetic resonance (MR) images (one DW image per gradient direction), making it time consuming. To reduce acquisition time while retaining the quality of estimation of the underlying structure, many compressed-sensing [2] approaches appear in recent works [3, 4, 5, 6].

Recent dictionary-based approaches [6] for HARDI reconstruction use sets of hundreds of atoms where, within a set, each atom varies only the orientation of the modeled tract(s) over a fixed finite set of orientations. While this strategy limits the accuracy of estimation of tract orientation to the fineness of the discretization, finer discretizations create atoms with high mutual coherence that decreases the reliability of identifying the correct atom and, hence, the tract orientation. This paper introduces the concept of a *rotation-invariant dictionary* that enables a concise dictionary (few atoms representing key diffusion-signal types) by explicitly optimizing the rotation for each atom during sparse fitting at every voxel.

Recent compressed-sensing approaches for HARDI subsample the set of gradient directions [3, 4, 6]. This strategy of acquiring full k-space for some directions and *no* k-space for others is somewhat imbalanced because it ignores *all* data associated with some directions. In contrast, the proposed framework generalizes acquisition schemes to enable a *balanced undersampling of k-space*, within all gradient directions' DW images. Echo planar imaging (EPI) with simultaneous image refocusing (SIR) [7] leads to fast clinical HARDI, without subsampling directions, allowing exploration of the proposed k-space undersampling schemes.

Unlike typical approaches that restrict diffusion-signal models to either frames alone (e.g. spherical ridgelets [3]) or dictionaries alone [6], the proposed framework models HARDI images using a novel *combination* of *frames* (overcomplete wavelet frame over space) *and dictionaries* (diffusion-signal values over gradient directions). The proposed joint modeling alleviates the need for large dictionaries that attempt to capture all intricate variations in the diffusion signal—probably impossible without a huge amount of training data. Moreover, unlike current approaches that enforces spatial regularization on the estimated DW images by penalizing their total variation [3], the proposed frame-based spatial model enforces *spatial regularity over multiple scales*.

2. ROTATION-INVARIANT DICTIONARIES FOR SPARSE CODING OF DIFFUSION SIGNALS

This section proposes (i) a novel model of a rotation-invariant dictionary for HARDI data, which enables concise dictionaries (few atoms) that retain, even enhance, the information captured in the dictionary in [6] and (ii) a novel method for sparse fitting the proposed dictionary model to HARDI data.

The authors gratefully acknowledge funding via NIH R01 EB00177.

Consider a dictionary model where each atom represents an uncorrupted single-voxel *diffusion signal* [1], i.e. DW values $S(g) \in \mathbb{R}$ for N gradient directions $g \in \{g_n \in \mathbb{S}^2\}_{n=1}^N$. The diffusion signal is a real-valued function on a (discretized) spherical domain. Because $S(g) = S(-g)$, HARDI acquires $S(g)$ for $\{g_n\}$ restricted to a hemisphere.

We propose a dictionary with a small number I of atoms $\{d_i \in \mathbb{R}^N\}_{i=1}^I$ that represent key types of diffusion profiles, e.g. a voxel with (i) isotropic diffusion, (ii) one moderately-anisotropic tract, (iii) one highly-anisotropic tract, (iv) two tracts crossing at 90°, (v) two tracts crossing at 60°, etc. Instead of including hundreds of atoms differing only in the orientation of the modeled tract(s) [6], the proposed dictionary model maintains only a single such atom and thereby (i) reduces the number of atoms in the dictionary by orders of magnitude, which can reduce computation time, and (ii) decreases the mutual coherence between the atoms leading to effective sparse coding [2]. Moreover, while the aforementioned multiple-rotated-atom-copies approach [6] suffers from discretization-related errors while estimating tract orientation, the proposed approach solves for an optimal tract orientation. Without loss of generality, to aid sparse coding, we (i) rescale the isotropic-diffusion atom to unit norm and (ii) shift and scale all other atoms to zero mean and unit norm.

Given an observed diffusion signal $s \in \mathbb{R}^N$ and the proposed dictionary $\{d_i\}_{i=1}^I$ (both use the same set of gradient directions $\{g_n\}_{n=1}^N$), we define the sparse-coding problem as:

$$\min_{\mathcal{R},c} \|s - \sum_i c_i \mathcal{R}_i(d_i)\|_2^2 \text{ such that } \|c\|_0 \leq \tau, \qquad (1)$$

where $\mathcal{R}_i(d_i) \in \mathbb{R}^N$ is the rotated atom d_i (precise definition within the next two paragraphs), $c \in \mathbb{R}^I$ where $c_i \in \mathbb{R}$ is the coefficient for the i^{th} rotated atom, $\|c\|_0 \triangleq \lim_{p\to 0} \|c\|_p^p$, and the constant $0 < \tau < I$ specifies the sparsity level.

We propose the following optimization algorithm: **(A)** initialize: $\forall i, c_i \leftarrow 1$, $\mathcal{R}_i(d_i) \leftarrow d_i$; **(B)** fix c, optimize $\mathcal{R}$; **(C)** fix $\mathcal{R}$, optimize c; **(D)** repeat (B)-(C) until converged.

In Step **(B)**, given coefficients c, we optimize to get rotated atoms $\{\mathcal{R}_i(d_i)\}$ as follows. First, we use point-reflection symmetry $s(g) = s(-g)$ to define a diffusion signal $\widehat{s}$ with the domain as the entire sphere (instead of a hemisphere), i.e. $\widehat{s} \in \mathbb{R}^{2N}$ where for $1 \leq n \leq N : \widehat{g}_n \triangleq g_n, \widehat{s}_n \triangleq s_n$ and for $(N+1) \leq n \leq 2N : \widehat{g}_n \triangleq -g_{n-N}, \widehat{s}_n \triangleq s_{n-N}$. Second, we define atoms $\{\widehat{d}_i\}$ on the entire sphere. Third, $\forall\ \widehat{d}_i$, we independently solve the following registration problem for the two functions $\widehat{s}(\cdot)$ and $\widehat{d}_i(\cdot)$ defined on $\mathbb{S}^2$:

$$R_i^{\text{opt}} \triangleq \arg \min_{R_i \in SO(3)} \sum_{n=1}^{2N} \left[\widehat{t}(g_n) - c_i \widehat{d}_i(R_i g_n)\right]^2, \qquad (2)$$

where $R_i \in \mathbb{R}^{3\times 3}$ is an orthogonal matrix and $\widehat{t} \triangleq \widehat{s} - \sum_{k\neq i} c_k \mathcal{R}_k(d_k)$ is the residual after subtracting the contributions of all other atoms k from the observed diffusion signal $\widehat{s}$. During this optimization, we obtain atom values $\widehat{d}_i(R_i g_n)$ at rotated gradient directions $R_i g_n$ via interpolation that relies on Barycentric coordinates using geodesics on $\mathbb{S}^2$. We optimize the orthogonal matrix R_i via projected gradient descent on the manifold $SO(3)$, which guarantees convergence to a local minimum. Finally, we get the diffusion signal corresponding to the optimally rotated i^{th} atom $e_i \triangleq \mathcal{R}_i(d_i)$ by the interpolated values $\{e_i(g_n) \triangleq \widehat{d}_i(R_i^{\text{opt}} g_n) : 1 \leq n \leq N\}$.

In Step **(C)**, given rotated atoms e_i, we optimize coefficients c by relaxing the $\|\cdot\|_0$ constraint to $\|\cdot\|_1$ and solving a robust-regression (Lasso) problem:

$$\min_c \|s - \sum_i c_i e_i\|_2^2 \text{ such that } \|c\|_1 \leq \tau. \qquad (3)$$

3. RECONSTRUCTION VIA JOINT FRAME-BASED AND DICTIONARY-BASED SPARSE MODELS

This section proposes a novel HARDI-reconstruction formulation that (i) enables flexible undersampling schemes in *both k-space and gradient directions*, thereby generalizing current schemes that ignore k-space undersampling within each DW-image scan; (ii) enables *concise* dictionaries having *rotation-invariant* atoms that capture key diffusion-signal types; and (iii) combines dictionaries with wavelet frames that enforce *multi-scale spatial regularity*, in addition to sparsity, on the estimated HARDI image.

Given undersampled HARDI data z (complex) associated with N gradient directions, and a concise rotationally-invariant dictionary with atoms $d_i \in \mathbb{R}^N$, we define the reconstructed HARDI image u^{opt} (complex) as:

$$\arg\min_u \min_{\mathcal{R},c,P} \Big[(1-\lambda) \sum_j \|u_j - P_j \sum_i c_{ji} \mathcal{R}_{ji}(d_i)\|_2^2 + \lambda \log(\|\Psi u\|_1 + \epsilon)\Big] \text{ s.t. } \|\widehat{F}u - z\|_2^2 \leq \eta; \forall j, \|c_j\|_0 \leq \tau, \quad (4)$$

where $\lambda \in [0,1]$ is a free parameter, Ψ is a tight-frame analysis transform (we use an overcomplete wavelet transform applied separately to each DW image), ϵ is a tiny positive constant, $u_j \in \mathbb{C}^N$ comprises DW signal values at the j^{th} voxel for all N gradient directions, P_j is a $N \times N$ diagonal matrix where each diagonal component is a unit-magnitude complex number capturing phase, $c_j \in \mathbb{R}^I$ comprises coefficients $c_{ji} \in \mathbb{R}$ for each rotated atom i that best fits u_j, $\mathcal{R}_{ji}(d_i)$ is the rotated i^{th} atom that best fits u_j, $\widehat{F}$ is the undersampled Fourier transform, and η is the noise variance.

We propose the following optimization scheme: **(a)** initialize: $\lambda \in (0,1)$, $u \leftarrow \widehat{F}^{\dagger} z$; **(b)** fix u, optimize $\mathcal{R}, c, P$; **(c)** fix $\mathcal{R}, c, P$, optimize u; **(d)** repeat (b)-(c) until converged.

In Step **(b)**, for each voxel j, the optimal value of the n^{th} diagonal element of the diagonal matrix P_j equals the n^{th} component of the complex vector u_j rescaled to unit magnitude, i.e. $u_j(g_n)/|u_j(g_n)|$; because the weighted sum of rotated atoms $\sum_i c_{ji} \mathcal{R}_{ji}(d_i)$ is purely real. Given this optimal P_j, optimizing $\mathcal{R}, c$ reduces to the sparse-coding problem

in Equation (1) (solved in Section 2) where the observed diffusion signal s is obtained by taking the magnitude of each component of u_j, i.e. for $1 \leq n \leq N : s(g_n) \triangleq |u_j(g_n)|$.

Step **(c)** entails minimizing a non-smooth function of u (i.e. $\lambda \log(\|\Psi u\|_1+\epsilon)+(1-\lambda)\sum_j \|u_j - P_j \sum_i c_{ji}\mathcal{R}_{ji}(d_i)\|_2^2$) over a convex constraint set (i.e. $\|\widehat{F}u - z\|_2^2 \leq \eta$). We solve this using the iteratively-reweighted l_1-analysis approach [2] where we solve each iteration using a fast-converging algorithm for non-smooth convex optimization [8]. Many reconstruction formulations include $\|\widehat{F}u - z\|_2^2$ in the objective function (basis pursuit denoising) at the cost of a free parameter (multiplier) that is usually harder to estimate than η.

4. VALIDATION USING SIMULATED HARDI

This section validates the proposed framework on a simulated phantom comprising two tracts, one horizontal and one vertical, crossing at 90°. Figures 1(a)-(b) show its uncorrupted HARDI image (16x16 voxels, 81 gradient directions), where diffusion-signal values $\{S(g_n)\}_{n=1}^{N=81}$ (colormap on right) at each voxel are shown on a discretized hemisphere $\{g_n \in \mathbb{S}^2\}_{n=1}^{N=81}$; black sticks centered at each g_n show the functional gradient vector $\nabla S(g)$ on $\mathbb{S}^2$ solely to aid visualization.

Figure 1(c) shows the pseudo-radial acquisition (13x undersampling) for each g_n; note that, for $3D$ objects, stacking the pseudo-radial pattern along the 3rd spatial dimension can lead to a standard 3D-MRI acquisition that acquires a set of axis-aligned lines along the 3rd dimension. $\mathcal{N}(0, \sigma^2)$ i.i.d. noise was added to real and imaginary k-space; the signal-to-noise ratio (defined as the largest signal magnitude among all DW images divided by σ) equals 7, mimicking highly-noisy real acquisitions [3, 5]. Figure 1(d) shows the typical variation of root-mean-squared error (RMSE) with λ suggesting that roughly-equal contributions ($\lambda \in [0.3, 0.7]$) from dictionary and wavelet models produce the best results. Figure 1(e) shows the reconstruction using a "sliding-window" scheme that we propose for HARDI by filling un-acquired k-space with that from the nearest acquired gradient direction on $\mathbb{S}^2$. Reconstructions from approaches using "sliding-window" (Figure 1(e)), dictionary only (Figure 1(f)), wavelet only (Figure 1(g)), and dictionary combined with total-variation penalty in space (Figure 1(h)) are poor. The proposed model, combining a dictionary of diffusion signals with an overcomplete wavelet frame in space, shows a perfect reconstruction (Figure 1(i)). A currently-popular acquisition scheme subsampling gradient directions only (Figure 1(j); 13x undersampling; we choose the directions for which to acquire data by farthest-point clustering on $\{g_n \in \mathbb{S}^2\}_{n=1}^{N=81}$) leads to a poor reconstruction (Figure 1(k)). Thus, a balanced k-space undersampling across all directions (Figure 1(i)) can be better than subsampling directions alone (Figure 1(k)).

Figure 2 compares reconstructions via *two* contrasting undersampling schemes that (i) require *similar acquisition times* and (ii) have standard axis-aligned k-space readouts. The reconstruction (Figure 2(b)) from undersampling purely in gradient directions (Figure 2(a)) and the reconstruction (Figure 2(d)) from undersampling purely in k-space (Figure 2(c)) both appear good with very low RMSEs.

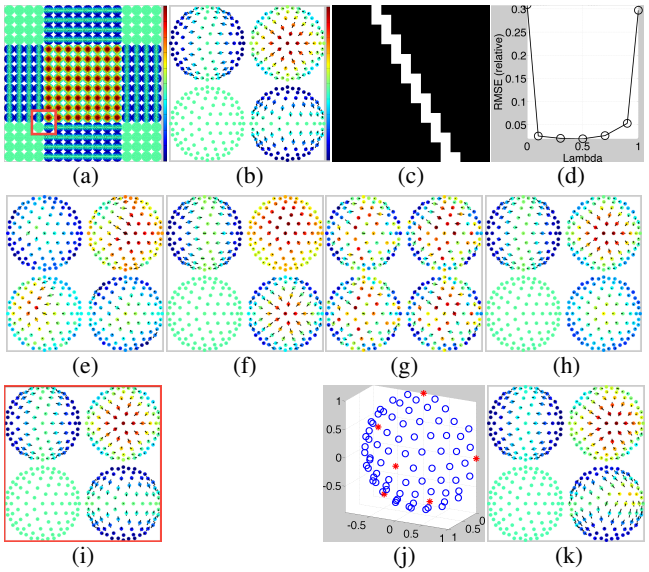

Fig. 1. Simulated-Phantom Reconstruction. (a) Uncorrupted diffusion signals $\{S(g_n)\}_{n=1}^{N=81}$ at all voxels. **(b)** Zoomed 2x2 region of interest boxed in lower-left part of (a). **(c)** Pseudo-radial k-space acquisition for one gradient direction; 13x undersampled k-space for all directions; k-space center ≡ image center; data acquired at bright pixels; other directions use randomly-rotated pattern. **(d)** Proposed method's performance with varying λ. **(e)** Reconstruction via "**sliding window**". **(f)** Reconstruction via **dictionary model**; λ = 0. **(g)** Reconstruction via **overcomplete-3D-wavelet (space-directions) model**; λ = 1. **(h)** Reconstruction via **combined dictionary and TV model**; λ = 0.5. **(i)** Reconstruction via **proposed combined dictionary and overcomplete-wavelet model**; λ = 0.5. **(j)** Subsampling 13x for gradient directions alone; directions shown on $\mathbb{S}^2$; Red-$*$ directions' k-space fully sampled; blue-$\circ$ directions ignored. **(k)** Reconstruction via **combined dictionary and overcomplete-wavelet model** for subsampled directions in (j); λ = 0.5.

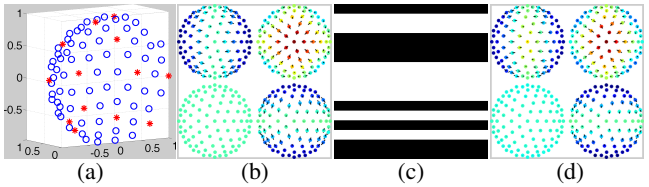

Fig. 2. Two Equally-Fast Undersampling Schemes; axis-aligned k-space readouts. **(a)** 6x subsampled directions; fully-sampled k-space for chosen directions. **(c)** 2x undersampled k-space for all directions; can use 4x SIR EPI [7]. **(b)** and **(d)** show similar-quality good reconstructions using (a) and (c), respectively, via proposed framework.

5. RESULTS USING CLINICAL BRAIN HARDI

This section shows the (i) utility of the proposed concise dictionary model and (ii) reconstructions via the proposed framework on undersampled clinical brain HARDI. We simulate undersampling on fully-sampled acquisitions: 108x108x40 2.5^3mm^3 voxels; 64 directions; b 2000 EPI MRI.

Figures 3(a)-(b) represent fully-sampled noisy data. Figures 3(c)-(e) show example atoms in the proposed rotation-invariant dictionary model (can be obtained from a different slice/dataset after denoising or fitting a multi-tensor model). Sparse dictionary fitting (proposed in Section 2) to noisy full data (Figure 4(a)) produces diffusion-signal estimates (Figure 4(c)) that closely match the underlying neural structure (Figure 4(b)) estimated by averaging within a small homogenous neighborhood. Dictionary fits to all voxels produces a generalized-fractional-anisotropy (GFA) map (Figure 4(d)) that has better contrast as compared to the GFA map (Figure 3(b)) obtained from noisy full data.

With undersampling both gradient directions and k-space, the proposed reconstruction framework produces GFA maps (Figure 5(b)-(d)) that are close to the benchmark GFA map in Figure 4(d). RMSEs between each GFA map in Figure 5(b)-(d) and the benchmark GFA map are all close to 0.21 (relative to 2-norm of the benchmark). The GFA map for "sliding-window" reconstruction (Figure 5(a)) is much blurrier; relative RMSE 0.3. Zooming into a crossing region, the proposed framework's reconstructed diffusion signals (Figure 6(d)) match those estimated from full data (Figure 6(b)) better than "sliding-window" reconstructions (Figure 6(c)).

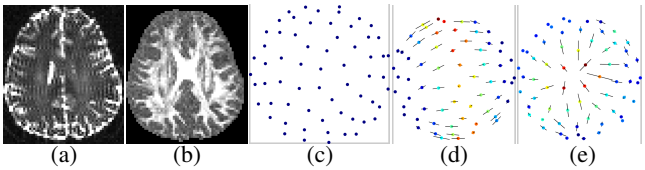

Fig. 3. **Rotation-Invariant Concise Dictionary Model. (a)** and **(b)** show B0 image and GFA map, respectively; axial slice of fully-sampled noisy data. **(c),(d),** and **(e)** show some dictionary atoms representing voxels with isotropic diffusion, single tract, and two crossing tracts, respectively.

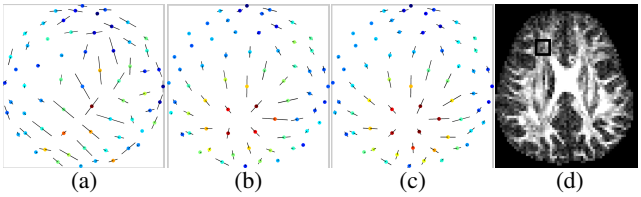

Fig. 4. **Sparse Fit of Dictionary Model to Data. (a)** Noisy fully-sampled data $\{S(g)\}$ at a voxel v with 2 crossing tracts. **(b)** Averaged signal in a 3x3 neighborhood of v. **(c)** Estimated signal at v by fitting the proposed dictionary model to (a); as per Section 2. **(d)** Estimated GFA by fitting proposed dictionary model at all voxels in slice in Figure 3(a)-(b).

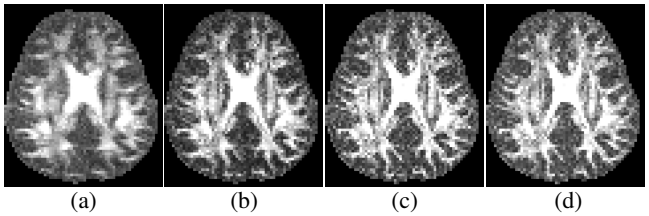

Fig. 5. **Undersampled Reconstruction – GFA Maps. (a)** "Sliding-window" scheme. **(b)** Proposed scheme; both (a) and (b) use 2x undersampled k-space for all gradient directions (can use SIR EPI [7]). **(c)** Proposed scheme; 1.5x subsampled directions; 1.33x undersampled k-space for acquired directions. **(d)** Proposed scheme; 2x subsampled directions; fully-sampled k-space for acquired directions.

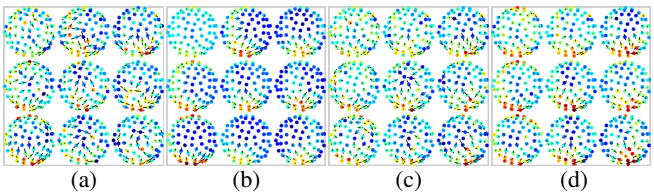

Fig. 6. **Undersampled Reconstruction – Crossing Region;** zoom into box in top left of Figure 4(d). **(a)** Noisy fully-sampled data. **(b)** Estimated signal by fitting dictionary to (a). **(c)** and **(d)** show reconstructions via "sliding-window" and the proposed scheme, respectively; 2x undersampled k-space for all directions (can use 4x SIR EPI [7]).

6. REFERENCES

[1] D Tuch, T Reese, and M Wiegell, "High angular resolution diffusion imaging reveals intravoxel white matter fiber heterogeneity," *Magn. Res. Med.*, vol. 48, no. 4, pp. 477–582, 2002.

[2] E. Candes and M. Wakin, "An introduction to compressive sampling," *IEEE Sig. Proc. Mag.*, pp. 21–30, 2008.

[3] O Michailovich, Y Rathi, and S Dolui, "Spatially regularized compressed sensing for high angular resolution diffusion imaging," *IEEE Trans. Med. Imag.*, vol. 30, pp. 1100–15, 2011.

[4] Y Rathi, O Michailovich, K Setsompop, S Bouix, M Shenton, and C-F Westin, "Sparse multi-shell diffusion imaging," in *Med. Imag. Comput. Comp. Assist. Interv.*, 2011, pp. 58–65.

[5] M Descoteaux, R Deriche, D LeBihan, J-F Mangin, and C Poupon, "Multiple q-shell diffusion propagator imaging," *Med. Imag. Anal.*, vol. 15, pp. 603–621, 2011.

[6] B Landman, J Bogovic, H Wan, F ElShahaby, P-L Bazin, and J Prince, "Resolution of crossing fibers with constrained compressed sensing using diffusion tensor MRI," *NeuroImage*, vol. 59, pp. 2175–2186, 2012.

[7] T Reese, T Benner, R Wang, D Feinberg, and V Wedeen, "Halving imaging time of whole brain diffusion spectrum imaging and diffusion tractography using simultaneous image refocusing in EPI," *J. Mag. Res. Imag.*, vol. 29, no. 3, pp. 517–22, 2009.

[8] Y. Nesterov, "Smooth minimization of non-smooth functions," *Math. Program., Ser. A*, vol. 103, pp. 127–152, 2005.